China Ocean Eng., 2017, Vol. 31, No. 3, P. 364–369
DOI: 10.1007/s13344-017-0043-0, ISSN 0890-5487
http://www.chinaoceanengin.cn/ E-mail: coe@nhri.cn

Study of Hydrodynamic Characteristics of A Sharp Eagle Wave Energy Converter

ZHANG Ya-qun[a, b, c, *], SHENG Song-wei[a, b, c], YOU Ya-ge[a, b, c], HUANG Zhen-xin[a, b, c], WANG Wen-sheng[a, b, c]

[a]Guangzhou Institute of Energy Conversion, Chinese Academy of Sciences, Guangzhou 510640, China

[b]CAS Key Laboratory of Renewable Energy, Guangzhou 510640, China

[c]Guangdong Provincial Key Laboratory of New and Renewable Energy Research and Development, Guangzhou 510640, China

Received April 20, 2015; revised November 3, 2015; accepted December 18, 2015

Abstract

According to Newton's Second Law and the microwave theory, mechanical analysis of multiple buoys which form Sharp Eagle wave energy converter (WEC) is carried out. The movements of every buoy in three modes couple each other when they are affected with incident waves. Based on the above, mechanical models of the WEC are established, which are concerned with fluid forces, damping forces, hinge forces, and so on. Hydrodynamic parameters of one buoy are obtained by taking the other moving buoy as boundary conditions. Then, by taking those hydrodynamic parameters into the mechanical models, the optimum external damping and optimal capture width ratio are calculated out. Under the condition of the optimum external damping, a plenty of data are obtained, such as the displacements amplitude of each buoy in three modes (sway, heave, pitch), damping forces, hinge forces, and speed of the hydraulic cylinder. Research results provide theoretical references and basis for Sharp Eagle WECs in the design and manufacture.

Key words: Sharp Eagle wave energy converter (WEC), hydrodynamics, capture width ratio, optimal external damping, optimization design

Citation: Zhang, Y. Q., Sheng, S. W. , You, Y. G., Huang, Z. X. , Wang, W. S., 2017. Study of hydrodynamic characteristics of a sharp eagle wave energy converter. China Ocean Eng., 31(3): 364–369, doi: 10.1007/s13344-017-0043-0

1 Introduction

In recent years, wave energy converters (WECs) have been developed rapidly. Oscillating body (OB) WECs include most styles, such as Power Buoy, AWS, Duck, and Sharp Eagle (Qin and Wu, 2013; Zhao and Shen, 2013).

The Sharp Eagle WEC is a new type of floating OB WEC researched and developed by Guangzhou Institute of Energy Conversion, Chinese Academy of Sciences. Because the shape of the WEC is similar to a sea hawk's head, it was named "Sharp Eagle WEC". The Sharp Eagle WEC has been studied deeply since 2010. By far, three types of WECs have been developed, Sharp Eagle I and II with the capacity of 10 kW and 100 kW respectively, and Sharp Eagle Ⅲ with the average output power amount of 50 kW. The Sharp Eagle I WEC has been deployed to Dawanshan waters of Zhuhai City in southern China since December 28 in 2012. It finished the sea trials on May 21, 2014, and trouble-freely worked for 1672 hours, which is the longest working time among all WECs in China. The Sharp Eagle II is under preparation and to be tossed at the same location as the former. Now the Sharp Eagle Ⅲ WEC is being built. Sheng et al. (2013, 2014) researched the advantages of the Sharp Eagle WECs. Zhang et al. (2014) introduced the model tests of the WECs. Technologies of the WEC on the aspects of status information acquisition and control are included in Wang et al. (2014). Chen et al. (2014a, 2014b) presented the structural damage of the WEC during the rotating-collision process. Among all published papers, only Sheng et al. (2013) made preliminary analysis for dynamics performance on the Sharp Eagle WEC.

The Sharp Eagle II WEC is an example in this paper. Mechanical models of every buoy are established by analyzing the coupling movement among three modes of each buoy (Feng et al., 2013). After calculating hydrodynamic parameters by numerical simulation method, the mechanical models and all forces are solved. Under the condition of

Foundation item: This work was financially supported by the National Natural Science Foundation of China (Grant No. 41406102) and the Special Foundation for Ocean Renewable Energy (Grant No. GHME2016YY01).

*Corresponding author. E-mail: zhangyq@ms.giec.ac.cn

the optimal external damping, design parameters of the Sharp Eagle II WEC are continuously optimized until an optimal design scheme is obtained.

2 Mathematical models

The structure of the Sharp Eagle II WEC is shown in Fig. 1. The WEC consists of three systems, a power capture system, a power take-off (PTO) system, and a mooring system. The power capture system includes two components, an Eagle head power prime mover (named Buoy 1) and an underwater appendage (named Buoy 2). The two are connected as a whole by a door hinge at Point C (on *xoy* plane). The rod ends of the hydraulic cylinders which belong to the PTO system are installed on Buoy 1 at Point A. The other ends are installed on Buoy 2 at Point B. The gravity centers of Buoy 1 and Buoy 2 are indicated by Point 1 and Point 2, respectively.

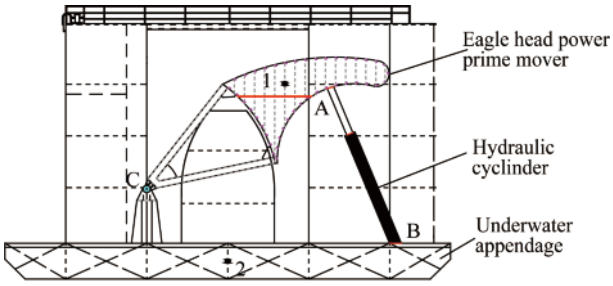

Fig. 1. Structure chart of Sharp Eagle WEC.

Assuming a total force for Buoy k is $F^{(k)}$ which includes a fluid force F_{f}, a damping force F_{C}, a still water recovery force F_{S}, a hinge force F_{J}, a buoyancy force, and a gravity force. Buoyancy force and the gravity force are a couple of balance forces, so they are disregard when calculating. There are 6-DOF movement modes which are sway, surge, heave, pitch, roll, and yaw (denoted by j=1, 2, ⋯, 6). Under the modes of pitch, heave and pitch, affections of the WEC are so obvious that the performances under the other modes are not taken into account.

Set the mass of Buoy k as $m^{(k)}$. According to Newton's Second Law, under j mode, we have

$$F_j^{(k)}(t) = m^{(k)}\ddot{X}_j^{(k)} = -\omega^2 m^{(k)} X_j^{(k)} \mathrm{e}^{-\mathrm{i}\omega t}. \tag{1}$$

By removing the time factor, $F_j(t)$ is decomposed, then

$$-\omega^2 m^{(k)} X_j^{(k)} = F_{\mathrm{f}j}^{(k)} + F_{\mathrm{C}j}^{(k)} + F_{\mathrm{J}j}^{(k)} + F_{\mathrm{S}j}^{(k)},\ j = 1,3,5, \tag{2}$$

where, $F_j^{(k)}$ and $X_j^{(k)}$ are total forces or torques and the displacements of buoy k under j mode, respectively; $F_{\mathrm{f}j}^{(k)}$, $F_{\mathrm{C}j}^{(k)}$, $F_{\mathrm{J}j}^{(k)}$, $F_{\mathrm{S}j}^{(k)}$ are the component forces of buoy k under j mode; ω is the round frequency of incident wave.

2.1 Forces equations

2.1.1 *Fluid force*

The fluid force acting on buoy k can be broken out as following:

$$F_{\mathrm{f}}^{(k)} = F_{\mathrm{w}}^{(k)} + F_{\mathrm{r}}^{(k)} \tag{3}$$

where, F_{w} is the wave excitation force for incident potential and diffraction potential; F_{r} is the wave radiation force for radiation potential.

The wave excitation force of buoy k under j mode, gained from Bernoulli equation, is

$$F_{\mathrm{w}j}^{(k)} = \iint_S \mathrm{i}\rho\omega(\Phi_{\mathrm{I}}^{(k)} + \Phi_{\mathrm{D}}^{(k)}) n_j \mathrm{d}s,\ j = 1,3,5. \tag{4}$$

The wave radiation force is:

$$F_{\mathrm{r}j}^{(k)} = \iint_S \mathrm{i}\rho\omega\Phi_{\mathrm{r}j}^{(k)} n_j \mathrm{d}s = \omega^2 m_{ji}^{(k)} X_j^{(k)} + \mathrm{i}\omega\mu_{ji}^{(k)} X_j^{(k)} \tag{5}$$

$$\begin{cases} m_{ji}^{(k)} = \iint_S \rho\mathrm{Re}(\varphi_{\mathrm{r}}{}^{j(k)}) n_j \mathrm{d}s \\ \mu_{ji}^{(k)} = \iint_S \rho\omega\mathrm{Im}(\varphi_r{}^{j(k)}) n_j \mathrm{d}s \end{cases} i,j = 1,3,5 \tag{6}$$

where, $\Phi_{\mathrm{I}}^{(k)}$, $\Phi_{\mathrm{D}}^{(k)}$ and $\Phi_{\mathrm{r}j}^{(k)}$ are the space velocity potentials of incident, diffraction and radiation of buoy k, respectively. $\phi_{\mathrm{r}}^{j(k)}$ is the unit radiation potential produced by unit velocity of buoy k under j mode; the density of the computational fluid is indicated by ρ; S is the wet surface; $m_{ji}^{(k)}$ and $\mu_{ji}^{(k)}$ are the added mass and the damping coefficient in j mode caused by the movement of mode i of buoy k.

2.1.2 *Damping force*

Damping force F_{C} overcomes the resistance of hydraulic oil to drive hydraulic cylinder for reciprocating motion. When the hydraulic cylinder moves, the damping force is viscous damping force (Kurniawan et al., 2012; Yang and Moan, 2011). Its value is proportional to the moving velocity, and has a direct influence on the amount of the output power. v_{A}, v_{B} and v_{ABL} are the velocity vectors of Point A, Point B, and the component of Point A relative to Point B along the line L, respectively. If F_{CA}, the damping force at Point A, is proportional to v_{ABL} along line L, then

$$F_{\mathrm{CA}} = -Cv_{\mathrm{ABL}}, v_{\mathrm{ABL}} = \sum_{j=1,3} (v_{\mathrm{A}j} - v_{\mathrm{B}j}) n_{jl}, \tag{7}$$

where, C is the external damping coefficient provided by viscous hydraulic oils; n_{jl} is the component of the unit vector under the mode of j along line L; $v_{\mathrm{A}j}$ and $v_{\mathrm{B}j}$ are the velocity components under j mode.

2.1.3 *Hinge force*

As shown in Fig. 1, the hinge force F_{J} acts on both buoys at the same Point C. So the velocity at Point C can be expressed by two equations:

$$\boldsymbol{v}_{\mathrm{C}} = \boldsymbol{v}_1 + \boldsymbol{\omega}_1 \times \boldsymbol{r}_{\mathrm{C1}}; \tag{8}$$

$$\boldsymbol{v}_{\mathrm{C}} = \boldsymbol{v}_2 + \boldsymbol{\omega}_2 \times \boldsymbol{r}_{\mathrm{C2}}. \tag{9}$$

As v_j=–iωX_j, j=1 or 3, we obtain:

$$-\mathrm{i}\omega_1 X_{11} + \omega_1 R_{\mathrm{C1,3}} = -\mathrm{i}\omega_2 X_{21} + \omega_2 R_{\mathrm{C2,3}}; \tag{10}$$

$$-\mathrm{i}\omega_1 X_{13}+\omega_1 R_{\mathrm{C1},1}=-\mathrm{i}\omega_2 X_{23}+\omega_2 R_{\mathrm{C2},1}, \quad (11)$$

where, $\boldsymbol{v}_1$, $\boldsymbol{v}_2$, and $\boldsymbol{v}_\mathrm{C}$, are the velocity vectors of Point 1, Point 2 and Point 3, respectively. r_{C1} and r_{C2} are the distance vectors between Point C and Point 1, Point C and Point 2; $R_{\mathrm{C1,\,3}}$ is the distance between Point C and Point 1 in the third mode, and the same with $R_{\mathrm{C2,\,3}}$, $R_{\mathrm{C1,\,1}}$ and $R_{\mathrm{C2,\,1}}$.

2.1.4 *Still water recovery force*

Still water recovery force $F_{\mathrm{S}j}^{(k)}$ comes from change of buoyancy when the WEC moves in the direction of the j-th mode. $F_{\mathrm{S}j}^{(k)}$ is

$$F_{\mathrm{S}j}^{(k)}=-\iint_S \rho g\eta \boldsymbol{n}\mathrm{d}s=-\rho g A(X_3-\eta), \quad (12)$$

where A is the water plane area, when buoy k is submerged fully, A=0.

2.2 Optimal design parameters

Within an incident wave period, the capturing energy and average power of the WEC are as follows:

$$w=-\int_0^T f_\mathrm{C}\mathrm{Re}[V_{\mathrm{ABL}}\mathrm{e}^{-\mathrm{i}\omega t}]\mathrm{d}t=C\int_0^T \mathrm{Re}[V_{\mathrm{ABL}}\mathrm{e}^{-\mathrm{i}\omega t}]^2\mathrm{d}t; \quad (13)$$

$$\begin{aligned}P&=\frac{w}{T}=\frac{C}{2}\left\{\mathrm{Re}[V_{\mathrm{ABL}}]^2+\mathrm{Im}[V_{\mathrm{ABL}}]^2\right\}\\&=\frac{C}{2}|V_{\mathrm{ABL}}|^2=\frac{C}{2}V_{\mathrm{ABL}}\overline{V}_{\mathrm{ABL}}.\end{aligned} \quad (14)$$

When the average power reaches the maximum value, the external damping is defined as the optimal one:

$$\begin{aligned}\left.\frac{\partial P}{\partial C}\right|_{C=C_{\mathrm{opt}}}&=\frac{1}{2}\left(V_{\mathrm{ABL}}\overline{V}_{\mathrm{ABL}}+C\frac{\partial V_{\mathrm{ABL}}}{\partial C}\overline{V}_{\mathrm{ABL}}\right.\\&\left.+CV_{\mathrm{ABL}}\frac{\partial \overline{V}_{\mathrm{ABL}}}{\partial C}\right)\Big|_{C=C_{\mathrm{opt}}}=0,\end{aligned} \quad (15)$$

where, w and P are the capturing energy and average power of the WEC, respectively. V_{ABL} and $\overline{V}_{\mathrm{ABL}}$ are a pair of conjugate values; C_{opt} represents the optimal external damping.

2.3 Capture width ratio

As the width of the Sharp Eagle WEC is B, the incident wave power is:

$$P_0=\rho g H^2\frac{\omega}{16m}\left[1+\frac{2mh}{\sinh(2mh)}\right]B. \quad (16)$$

With Eq. (12), when C=C_{opt}, the optimum capture width ratio for the WEC is:

$$\eta=\frac{P_{\mathrm{opt}}}{P_0}, \quad (17)$$

where, P_0 is the incident waves power; η is the capture width radio; g, H, m and B are the gravitational acceleration, height of incident wave, wave number and width of the WEC facing to incident waves, respectively.

3 Results of numerical simulation

Based on Eqs. (3)–(5), three hydrodynamic parameters are obtained when the WEC is acting on unit amplitude incident waves, such as the added masses (Morison et al., 1953), damping coefficients, and wave forces or torques (Sabuncu and Calisal, 1981; Calisal and Sabuncu, 1984; Kaye and Maull, 1993; Bhatta and Rahman, 2003).

3.1 Added mass

The added masses are proportional to the area of a buoy to impede the movement of water particle. Therefore, the larger the added mass under one mode is, the larger the inertia is. Figs. 2 and 3 show the added masses of buoys under three modes, respectively. All the added masses of Buoy 1 are smaller than those of Buoy 2. Both buoys have small added masses for the pitch mode.

3.2 Damping coefficients

The damping coefficient is a coefficient of a damping force acting on a WEC when it is capturing wave energy. The damping coefficient is proportional to the resistance. Figs. 4 and 5 show the damping coefficients of the two buoys, respectively. All the values of Buoy 2 are larger than

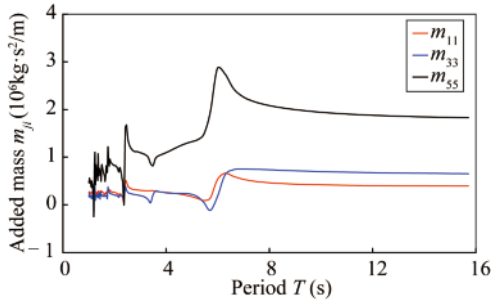

Fig. 2. Added mass of Buoy 1.

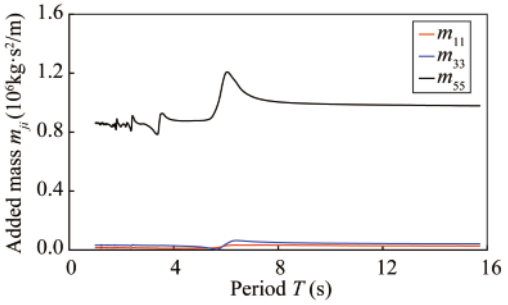

Fig. 3. Added mass of Buoy 2.

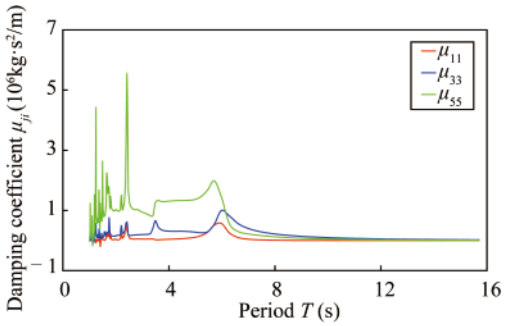

Fig. 4. Damping coefficient of Buoy 1.

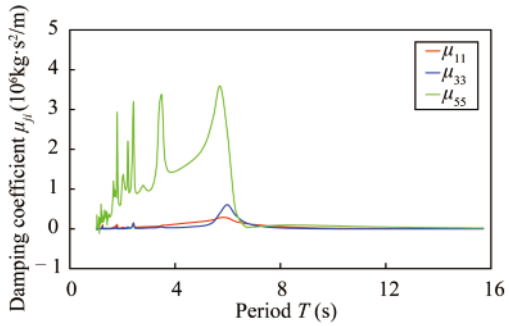

Fig. 5. Damping coefficient of Buoy 2.

those of Buoy 1 in three modes. The damping coefficients of the two buoys under the mode of the pitch are the largest, but those of the other two modes almost reach zero.

3.3 Fluid force and torques

Fig. 6 shows fluid forces (or torques) curves of two buoys in three modes under the action of incident waves with unit wave amplitude. The forces (or torques) of Buoy 1 are larger than those of Buoy 2. So the former could move much easier than the latter, and Buoy 2 could keep stable.

4 Optimization design

Based on Eqs. (13)–(15), if the external damping coefficients change from 100000 Ns/m to 800000 Ns/m, the curves of the capture width ratio are as shown in Fig. 7. The capture width ratio trends to converge to zero within the period 0–16 s. Since the WEC could capture larger energy in every period, we choose C_{opt}=300000 Nm/s as the optimal external damping coefficient, and the curve of optimal capture width ratio is shown in Fig. 8.

Figs. 9–14 show curves of some parameters when C_{opt}=300000 Nm/s, such as the motion amplitude, hinge forces, damping forces, and the speed of the hydraulic cylinder. The maxima of all data occur at about T=6 s which is the common cycle for incident waves in Dawanshan waters.

Figs. 9–11 show that the displacement of Buoy 1 is larger than that of Buoy 2 in the same mode. In different modes, for Buoy 1, the longer the period of the incident

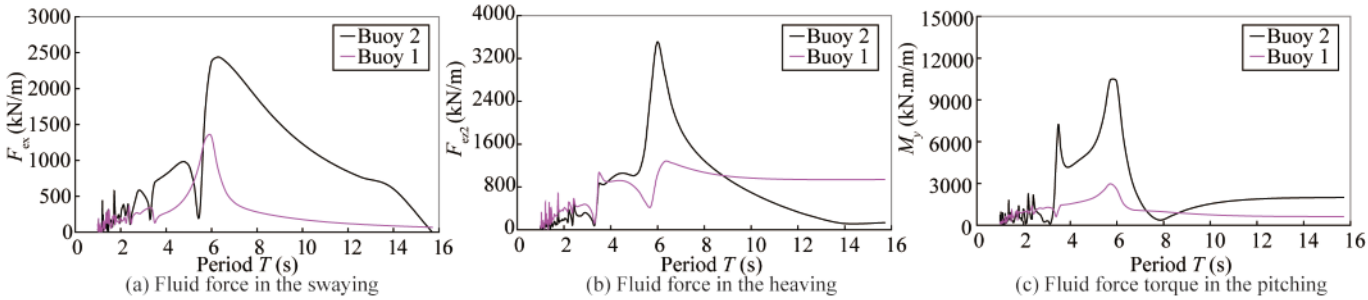

Fig. 6. Force and torque in different motion modes.

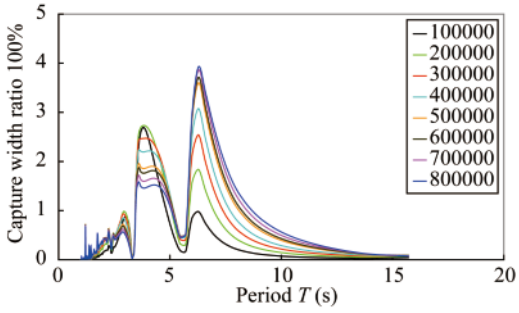

Fig. 7. Capture width ratio of different outer damping.

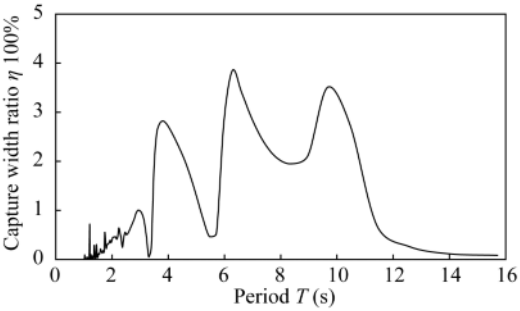

Fig. 8. Optimal capture width ratio.

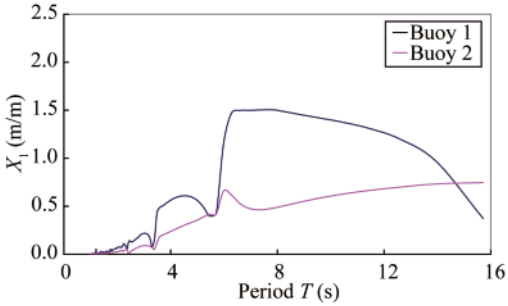

Fig. 9. Displacement amplitude in sway.

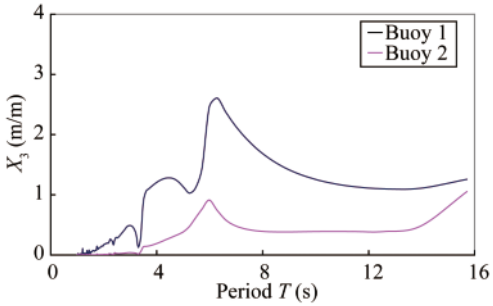

Fig. 10. Displacement amplitude in heave.

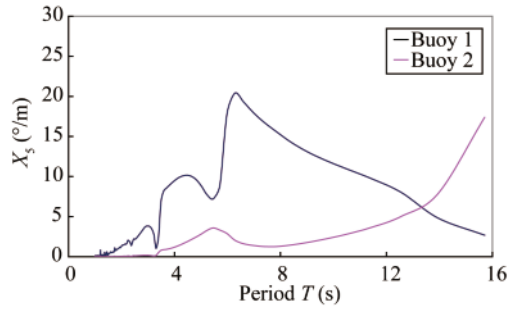

Fig. 11. Angle amplitude in pitch.

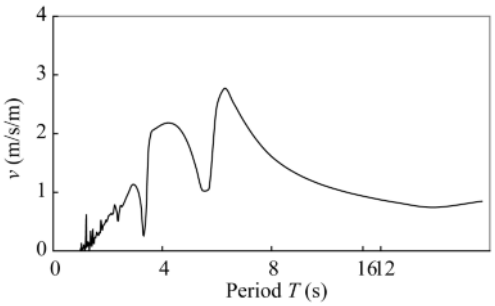

Fig. 14. Velocity of the hydraulic cylinder.

wave is, the larger the movement amplitude is. But for Buoy 2, when the period of the incident waves increases, the movement amplitude falls down after reaching the peak. Acted under unit amplitude incident waves to pitch, the maximum angle difference between the two buoys is up to 20.92°, and the maximum displacement in the heave is almost twice the one in the sway.

Fig. 12 shows two components of the hinge force. One is under heave mode, and the other is under sway mode. The difference of the values of the two forces is very slight, and the trends of both are similar which increase firstly, decrease later, and finally stay stable. The peaks of the two are F_{Jx}=1910.3 kN and F_{Jz}=898.3 kN.

Figs. 13 and 14 show the damping force and the velocity of the hydraulic cylinder, respectively, both of which are under the condition of the optimal external damping coefficient. The speed is linearly proportional to the damping force. The two parameters have the same change processes that rise and fall for three times. At T=6.28 s, the

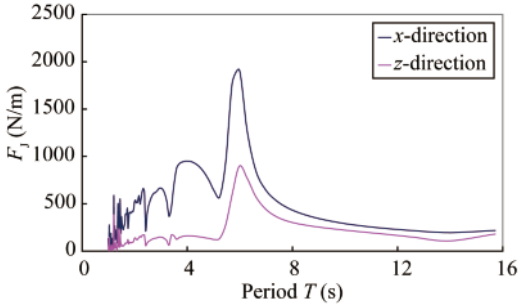

Fig. 12. Hinge forces.

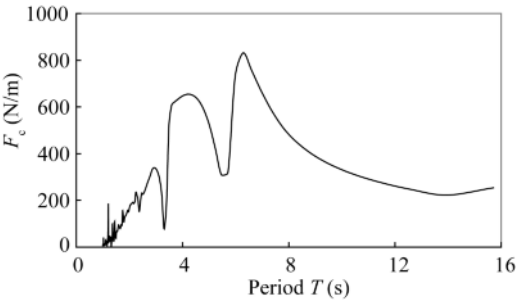

Fig. 13. Damping force.

maximum damping force is F_{Cmax}=831.42 kN and the maximum velocity of the hydraulic cylinder is v_{max}=2.77 m/s.

5 Conclusions

This paper introduces hydrodynamic research on Sharp Eagle II WEC. The work includes setting up mechanical model with numerical simulation, and obtaining the optimum additional damping coefficient and optimal capture width ratio to determine the optimized design. According to the above research, the following conclusions can be drawn:

(1) The WEC has a good response on a wide range of incident wave frequency, and shows especially better hydrodynamic performances at the period of 4–8 s.

(2) The underwater appendage achieves the design effect as a stable structure when the WEC is capturing wave energy.

(3) The Eagle head power prime mover has a strong ability to capture wave energy. Under the unit wave amplitude of the incident wave, the maximum angle between the Eagle head power prime mover and the underwater appendage is up to 20.92 ° in pitch.

(4) The WEC can efficiently capture wave energy. When the optimal external damping is C_{opt}=300000 Nm/s, the conversion efficiency gains the highest value η=385%, with the incident wave period of 6.28 s.

References

Bhatta, D.D. and Rahman, M., 2003. On scattering and radiation problem for a cylinder in water of finite depth, *International Journal of Engineering Science*, 41(9), 931–967.

Calisal, S.M. and Sabuncu, T., 1984. Hydrodynamic coefficients for vertical composite cylinders, *Ocean Engineering*, 11(5), 529–542.

Chen, A.J., You, Y.G., Sheng, S.W. and Peng, W., 2014a. Damage analysis of eagle wave energy converter in rotating-collision, *Advances in New and Renewable Energy*, 2(2), 129–134. (in Chinese)

Chen, A.J., You, Y.G., Sheng, S.W. and Peng, W., 2014b. Study on the structural damage of the eagle type wave energy converter due to the rotating-collision process, *Journal of Ocean Technology*, 33(4), 6–11. (in Chinese)

Feng, P.Y., Ma, N. and Gu, J.C., 2013. Research on wave energy recovery by oscillating wings for energy efficient ship propulsion, *Journal of Ship Mechanics*, 17(9), 1021–1030.

Kaye, D. and Maull, D.J., 1993. The response of a vertical cylinder in waves, *Journal of Fluids and Structures*, 7(8), 867–896.

Kurniawan, A., Pedersen, E. and Moan, T., 2012. Bond graph modelling of a wave energy conversion system with hydraulic power takeoff, *Renewable Energy*, 38(1), 234–244.

Morison, J.R., Johnson, J.W. and O'Brien, M.P., 1953. Experimental studies of forces on piles, *Coastal Engineering Proceedings*, 1(4), 25.

Qin, L. and Wu, B.J., 2013. Oscillating properties of a wave energy device consisting of double cylindrical floats, *Journal of Ship Mechanics*, 17(11), 1253–1261. (in Chinese)

Sabuncu, T. and Calisal, S., 1981. Hydrodynamic coefficients for vertical circular cylinders at finite depth, *Ocean Engineering*, 8(1), 25–63.

Sheng, S.W., You, Y.G. and Wang K.L., 2013. Research on 10kW sharp eagle wave energy convertor, *The 2nd Session of the China Marine Renewable Energy Development Forum Annual Meeting Proceedings*, National Ocean Technology Center, Guangzhou, 378–384. (in Chinese)

Sheng, S.W., You, Y.G. and Wang, K.L., 2014. *Research and Development of Sharp Eagle Wave Energy Convertor*, Report of 5th International Conference on Ocean Energy, Halifax, Canada.

Wang, K.L., Sheng, S.W., You, Y.G., Zhang, Y.Q., Jiang, J.Q., Lin, H.J. and Ye, Y., 2014. Research on the redundancy monitoring system of the "Sharp Eagle No.l" floating wave energy converter, *Journal of Ocean Technology*, 33(4), 62–67. (in Chinese)

Yang, L.M. and Moan, T., 2011. Dynamic analysis of wave energy converter by incorporating the effect of hydraulic transmission lines, *Ocean Engineering*, 38(16), 1849–1860.

Zhang, Y.Q., Sheng, S.W., You Y.G., Wang, Z.P., Wang, K.L, and Lin, H.J., 2014. Experimental study on a 100 kW one-base multi-buoy floating "Sharp Eagle" wave energy converter, *Journal of Ocean Technology*, 33(4), 73–80. (in Chinese)

Zhao, H.T. and Shen, J.F., 2013. An experimental study on hydrodynamic performance of a bottom-hinged flap wave energy converter, *Journal of Ship Mechanics*, 17(10), 1097–1106. (in Chinese)